Article

Discovery Medicine 2025; 37(197): 1023–1032
https://doi.org/10.24976/Discov.Med.202537197.91

Mechanism of AGT-Mediated Magnesium Ion Uptake in Age-Related Olfactory Dysfunction

Dong Wang[1,2], Jinxiong Yang[1], Bo Liu[2], Wenlong Luo[1,*]

[1]Department of Otolaryngology-Head and Neck Surgery, The Second Affiliated Hospital of Chongqing Medical University, 400010 Chongqing, China
[2]Department of Otolaryngology-Head and Neck Surgery, The Central Hospital of Dazhou, 635000 Dazhou, Sichuan, China
*Correspondence: luowenlong@hospital.cqmu.edu.cn (Wenlong Luo)
Published: 9 June 2025

Background: Ageing is associated with a significant decline in olfactory function, though the underlying mechanisms remain unclear. Angiotensinogen (AGT) participates in multiple cellular processes, including inflammation, oxidative stress (OS), and magnesium (Mg^{2+}) homeostasis. In this study, we investigated how decreased AGT expression in olfactory epithelial cells affects Mg^{2+} uptake, inflammation, oxidative stress, and mitochondrial apoptosis, ultimately contributing to olfactory dysfunction.
Methods: Rapidly ageing male senescence-accelerated mouse prone 6 (SAMP6) mice and age-matched normal senescence accelerated mouse resistant 1 (SAMR1) control mice were used to evaluate olfactory function via the buried food test. Blood and olfactory epithelium tissues were collected for biochemical analyses. Mouse olfactory epithelial (MOE) cells were cultured, and AGT expression was knocked down, with or without $MgSO_4$ supplementation. Mitochondrial membrane potential ($\Delta\Psi m$) was assessed using JC-1 staining, and cell viability was measured via Cell Counting Kit-8 (CCK-8) assay.
Results: SAMP6 mice exhibited impaired olfactory function, with significant structural damage to the olfactory epithelium and reduced expression of olfactory marker protein (OMP, $p < 0.05$). Elevated expression of interleukin-1 beta (IL-1β), tumor necrosis factor alpha (TNF-α), transforming growth factor beta (TGF-β), reactive oxygen species (ROS), Bcl-2-associated X protein (Bax), caspase-3, and caspase-9 was observed in blood and olfactory epithelium tissues, while levels of AGT, Angiotensin II (Ang II), Mg^{2+}, and the Mg^{2+} transporter mitochondrial RNA splicing 2 protein (MRS2) and transient receptor potential cation channel subfamily M member 6 (TRPM6) were significantly decreased ($p < 0.05$). *In vitro*, AGT knockdown reduced viability and $\Delta\Psi m$ in MOE cells ($p < 0.05$), elevated IL-1β, TNF-α and ROS ($p < 0.05$), and suppressed the expression of AGT, Ang II, MRS2, and TRPM6 ($p < 0.05$). Notably, $MgSO_4$ administration partially reversed the effects of AGT knockdown on MOE cells ($p < 0.05$).
Conclusion: Reduced AGT expression in olfactory epithelial cells impairs Mg^{2+} uptake, leading to inflammation, oxidative stress, and mitochondrial apoptosis, ultimately contributing to age-related olfactory dysfunction. Our findings suggest that targeting AGT or Mg^{2+} homeostasis may offer promising therapeutic strategies for age-related olfactory disorders.

Keywords: AGT; olfactory disorders; olfactory epithelial cells; Mg^{2+} uptake; apoptosis

Introduction

Olfactory disorders refer to a reduction or complete loss of the sense of smell. Ageing is a significant risk factor for olfactory dysfunction [1], and its prevalence has been notably documented in conditions such as Alzheimer's and Parkinson's disease [2]. However, recent study suggested that younger individuals may also exhibit age-like declines in olfactory function [3]. Moreover, the sense of smell is essential for daily activities, including food selection and detection of environmental hazards [4]. A decline in olfactory function can adversely impact patients' quality of life to varying degrees.

Generally, olfactory disorders arising from the nasal cavity and paranasal sinuses can be classified as either respiratory or sensory in origin. However, many related disorders result from a combination of contributing factors [5,6]. Consequently, it is widely accepted that, beyond mechanical obstruction in the olfactory cleft, inflammation in the olfactory cleft is a significant contributor to olfactory dysfunction associated with nasal cavities and sinus disorders [7,8]. Olfactory epithelial cells, primarily located within the olfactory cleft and containing olfactory receptors, serve as the primary sensory receptor cells for olfaction [9]. Therefore, abnormal functional phenotypes of olfactory epithelial cells are critical contributors to the decline in olfactory function.

The *Agt* gene encodes angiotensinogen [10], which plays a critical role in regulating inflammation, fibrosis, oxidative stress, and Mg^{2+} influx through its interaction with downstream receptors following the hydrolysis of angiotensin I to IV (Ang I–IV) [11–13]. Transcriptomic analyses of mouse olfactory epithelial cells have revealed a significant decrease in AGT expression in aged speci-

mens. Additionally, emerging evidence suggests that angiotensinogen (AGT) and related factors may be involved in olfactory dysfunction observed in COVID-19 patients, as angiotensin-converting enzyme 2 (ACE2), another component of the renin-angiotensin system (RAS), facilitates severe acute respiratory syndrome coronavirus 2 (SARS-CoV-2) entry and is associated with olfactory loss [14,15]. Notably, angiotensinogen/angiotensin II (AGT/Ang II) signaling and its associated receptors are involved in regulating cellular Mg^{2+} uptake [13], and magnesium is essential for maintaining sensitivity to smell and taste [16]. However, the specific role of AGT in olfactory disorders, particularly in relation to Mg^{2+} uptake, remains inadequately elucidated.

In this study, we investigated the role of AGT in olfactory epithelial cell function using the senescence-accelerated mouse prone 6 (SAMP6) mouse model of accelerated ageing. We confirmed that SAMP6 mice show olfactory deficits alongside downregulated *AGT* expression, reduced Mg^{2+} transporters, elevated inflammatory and oxidative stress markers, as well as increased mitochondrial apoptosis. Through *in vitro* knockdown of AGT in mouse olfactory epithelial (MOE) cells, we evaluated whether $MgSO_4$ supplementation could mitigate the inflammatory and apoptotic outcomes of AGT deficiency. Our findings provide new insights into the AGT-Mg^{2+} regulatory axis and may inform therapeutic strategies for age-related olfactory dysfunction.

Materials and Methods

Olfactory Function Evaluation

A total of 12 male specific-pathogen-free (SPF) mice used, including senescence-accelerated mouse prone 6 (SAMP6) mice (n = 6, aged 3–6 months, body weight = 32 $\pm$ 1.2 g) and age-matched senescence accelerated mouse resistant 1 (SAMR1) control mice (n = 6, aged 3–6 months, body weight = 30 $\pm$ 0.9 g), were obtained from Huachuang Sino (Taizhou, China). All mice underwent a 1-week acclimatization period before testing. Olfactory function was assessed using the buried food test. Mice were individually placed in a test box (40 cm $\times$ 24 cm $\times$ 20 cm) for 30 minutes per day over 3 consecutive days to acclimate to the test environment. Prior to the formal testing, mice were fasted for 12 hours. Approximately 3 cm of bedding material was added to the test box, and 0.5 g of food pellets were buried at a depth of 0.5 cm in a random location. Each mouse was placed in the box, and the timing started immediately. The time was recorded once the mouse uncovered the food pellet and grasped it using either its forepaws or teeth. Each mouse underwent three trials, and the average value was recorded. If a mouse failed to find the food within 300 seconds, the trial was terminated, and the search time was recorded as 300 seconds. Fresh bedding material was used for each trial to prevent odor cues.

Collection of Olfactory Epithelial Tissue and Blood Samples

One day after the completion of the olfactory function test, all mice were fasted for 8 hours and anesthetized via intraperitoneal injection of sodium pentobarbital (40 mg/kg; BC1040, Protein Biotechnologies, Beijing, China). Blood samples were collected from the orbital sinus. Mice were then euthanized via carbon dioxide asphyxiation using an experimental animal asphyxiator (DW800, Rurui Tech, Guangzhou, China). The nasal septum was dissected to separate the olfactory epithelium, including the nasal tip, septum, and mucosal surface of the nasal turbinates. The olfactory epithelium tissues were washed with PBS and either stored at –80 °C or fixed in 10% formaldehyde for subsequent analysis.

All animal experiments complied with the ARRIVE guidelines and were conducted in accordance with the National Institutes of Health Guide for the Care and Use of Laboratory Animals (NIH Publications No. 8023, revised 1978). Ethical approval was granted by the Institutional Animal Care and Use Committee of the Second Affiliated Hospital of Chongqing Medical University (approval number: IACUC-SAHCQMU-2023-0070).

Biochemical Detection

Collected blood samples were centrifuged at 8000 rpm for 20 minutes to separate serum. Serum samples were preserved on dry ice and shipped to the Central Laboratory of the Second Affiliated Hospital of Chongqing Medical University (Chongqing, China) for analysis. Levels of AGT, Ang II, Mg^{2+}, interleukin-1 beta (IL-1β), tumor necrosis factor alpha (TNF-α), transforming growth factor beta (TGF-β), reactive oxygen species (ROS), malondialdehyde (MDA), and superoxide dismutase (SOD) were quantified using a Toshiba automatic biochemical analyzer (TBA-120FR, Toshiba, Tokyo, Japan), following the manufacturer's instructions.

Pathological Observation

Olfactory epithelial tissues were fixed in 10% formaldehyde (BL539A, Biosharp, Hefei, China) for 24 hours, decalcified in 10% EDTA (798641, Sigma, St. Louis MO, USA), embedded in paraffin, and sectioned into 4 µm slices using a Leica RM2235 microtome (Leica Biosystems, Wetzlar, Germany). For hematoxylin and eosin (H&E) staining, sections were stained with hematoxylin for 3 minutes and eosin for 1 minute, followed by dehydration and mounting in neutral resin (C0105S, Beyotime, Shanghai, China). Images were captured using an OLYMPUS microscope (IX71, Tokyo, Japan) at 200$\times$ magnification (scale bars indicated).

Immunohistochemistry

Paraffin-embedded olfactory epithelial tissue sections were deparaffinized, rehydrated, and subjected to antigen retrieval with the repair solution (C1032, Solarbio, Beijing, China) at 98 °C for 20 minutes. Sections were then incubated in 3% H_2O_2 (SI125-01, SEVEN BIO, Beijing, China) at room temperature (RT) for 20 minutes. Following PBS washing, the sections were treated with 0.1% Triton X-100 for 10 minutes and incubated overnight at 4 °C with diluted olfactory marker protein (OMP) antibody (1:200, DF13678, INTERLAB, Beijing, China). Afterwards, sections were incubated with goat anti-rabbit IgG-HRP (1:200, PV9000, zsbio, Beijing, China) for 1 hour at 37 °C in the dark. DAB solution (KGP1045-20, keyGEN, Nanjing, China) was applied for 15 minutes, and nuclei were counterstained with hematoxylin for 10 minutes. Stained sections were observed under a microscope (OLYMPUS IX71, Tokyo, Japan).

Cell Culture and Treatment

Mouse olfactory epithelial (MOE) cells (CP-M149, Pricella, Wuhan, China) were cultured in DMEM medium supplemented with 10% FBS and 1% penicillin-streptomycin under standard conditions and verified as mycoplasma-free. MOE cells displayed typical epithelial morphology, including a cobblestone-like appearance with tightly packed polygonal shapes, clear cell borders, and centrally located nuclei. Lipofectamine 2000 (Invitrogen, 11668-019, Waltham, MA, USA) was used to transfect cells with short hairpin RNA targeting AGT (sh-AGT) or negative control (sh-NC), both prepared in serum-free medium. Cells were seeded at 60–70% confluence and transfected with 2 µg/mL sh-RNA plasmid complexes for 12 hours in serum-free DMEM, followed by complete medium replenishment. Cells were harvested after 48 hours to determine transfection efficiency via RT-PCR. To investigate the effect of Mg^{2+}, cells were treated with various doses of $MgSO_4$ (HY-Y1267D, MCE, Monmouth Junction, NJ, USA) (0, 1.25, 2.5, 5, and 10 mg/mL) for 48 hours. The shRNA target sequences are listed below:

sh-AGT-1: GAGGCAAATCTGAACAACATT;
sh-AGT-2: CCAAGGAACGATGAGAGGTTT;
sh-AGT-3: CCGCATGTACAAGATGCTGAA;
sh-NC: TTCTCCGAACGTGTCACGT.

RT-PCR

Total RNA was extracted from MOE cells using TRIzol and quantified using a NanoDrop spectrophotometer (840-317500, Thermo Fisher, Waltham, MA, USA). 1 µg RNA was reverse transcribed to cDNA using the FastKing RT Kit (KR116, Vazyme, Nanjing, China). RT-qPCR was performed using 1.2 µL of cDNA with the LightCycler 480 SYBR Green I Master mix (1725122, Bio-Rad, Hercules, CA, USA). *β-actin* was used as the internal reference gene. Relative mRNA expression levels were calculated using the $2^{-\Delta\Delta CT}$ method. The primer sequences were:

Agt-F, 5′-TGCTGAATGAGGCAGGAAGTGG-3′;
Agt-R, 5′-AGGGCAGCGAGGACCTTGTG-3′;
β-actin-F, 5′-GTCCCTCACCCTCCCAAAAG-3′;
β-actin-R, 5′-GCTGCCTCAACACCTCAACCC-3′.

Detection of Cell Viability

Cell viability was assessed using the Cell Counting Kit-8 (CCK-8) regent (A311-02, Vazyme, Nanjing, China). Mouse olfactory epithelial cells were seeded in 96-well plates (5×10^3 cells/well) and treated with $MgSO_4$ for 24 hours. Subsequently, 10 µL of CCK-8 solution was added to each well and incubated at 37 °C for 4 hours. Absorbance at 450 nm was recorded using a Thermo Multiscan MK3 (lot. K3, Waltham, MA, USA). Cell viability was calculated as (OD treated / OD control) × 100%.

Western Blotting

Proteins were extracted from the olfactory epithelial tissues and MOE cells using RIPA buffer (P0013C, Beyotime, Shanghai, China) and quantified using a BCA protein assay kit (P0010, Beyotime, Shanghai, China). A total of 35 µg of protein per sample was separated by SDS-PAGE gel and transferred onto PVDF membranes. Membranes were blocked with 5% skim milk for 1 hour at RT, followed by overnight incubation at 4 °C with the following primary antibodies: anti-AGT (1:400, DF7976, INTERLAB, Taibei, China), anti-Ang II (1:500, 11992-1-AP, Proteintech, Rosemont, IL, USA), anti-AT1R (1:500, 66415-1-Ig, Proteintech), anti-MRS2 (1:200, bs-17836R, BIOSS, Beijing, China), anti-TRPM6 (1:300, YN7418, Immunoway, Plano, USA), anti-Caspase-3 (1:1000, bs-0081R, BIOSS, Beijing, China), anti-Caspase-9 (1:1000, A18676, Abclonal, Wuhan, China), anti-IL-1β (1:1000, A16288, Abclonal), anti-TNF-α (1:1000, A24214, Abclonal), anti-Bax (1:400, 50599-2-Ig, Proteintech), anti-Bcl-2 (1:400, 12789-1-AP, Proteintech), and anti-β-actin (1:3000, AC038, Abclonal). After washing, membranes were incubated with goat anti-rabbit IgG-HRP (1:5000, AS014, Abclonal) or goat anti-mouse IgG-HRP (1:5000, AS003, Abclonal) at RT for 2 hours. Signal detection was performed using an ECL reagent (#34580, Thermo Fisher, Waltham, USA), and bands were visualized with a Tanon ChemiDoc 5200T system (Tanon, Shanghai, China). The grayscale intensity of each band was quantified using ImageJ software (NIH, Bethesda, MD, USA).

JC-1 Staining

JC-1 staining was used to evaluate mitochondrial membrane potential (MMP). Cells were incubated with the JC-1 probe (C2003S, Beyotime, Shanghai, China) and DAPI (C0065, Solarbio, Beijing, China) at 37 °C for 20 minutes in the dark after rinsing with PBS (P1020, Solarbio, Beijing, China). Unbound dye was removed by washing

with PBS, and fluorescence was observed using a confocal microscope (IX71, OLYMPUS, Tokyo, Japan). Changes in MMP were evaluated based on the red-to-green fluorescence intensity ratio.

Statistical Analysis

Data were analyzed using GraphPad Prism 8 (GraphPad Software, Inc., San Diego, CA, USA) and presented as mean ± standard deviation (SD). Differences between the two groups were assessed using the unpaired student's *t*-test. One-way analysis of variance (ANOVA) followed by Tukey's post hoc test was used for comparisons among multiple groups. A p-value < 0.05 was considered statistically significant.

Results

SAMP6 Mice Exhibited Decreased Olfactory Function and Reduced AGT Expression

Firstly, we examined whether there were differences in olfactory function between SAMP6 and SAMR1 mice. In the olfactory foraging test, SAMP6 mice required significantly more time to locate food than SAMR1 mice ($p < 0.05$, Fig. 1A), indicating hyposmia in SAMP6 mice. Histopathological examination revealed that the olfactory mucosal epithelial layer in SAMR1 mice was intact, with normal distribution of the olfactory mucosa and lamina propria. In contrast, SAMP6 mice exhibited atrophy of the olfactory mucosal epithelial layer, along with reduced thickness of the epithelium and lamina propria (Fig. 1B). Immunohistochemistry (IHC) analysis showed that the expression of the olfactory marker protein OMP was significantly lower in the olfactory epithelium of SAMP6 mice than in SAMR1 mice ($p < 0.05$, Fig. 1C). Additionally, SAMP6 mice displayed a significant decrease in serum SOD content and a significant increase in IL-1β, TNF-α, TGF-β, ROS, and MDA levels ($p < 0.05$, Fig. 1D,E). Moreover, serum levels of AGT, Ang II, and Mg^{2+} were significantly reduced in SAMP6 mice compared to SAMR1 mice ($p < 0.05$, Fig. 1F).

SAMP6 Mice Showed Altered Expression of Proteins Related to AGT, Mg^{2+} Transport, Inflammation, and Mitochondrial Apoptosis in the Olfactory Epithelium

Next, we analyzed the expression of inflammation-related proteins in the olfactory epithelium of SAMP6 mice and SAMR1 mice. The results showed significantly elevated levels of IL-1β and TNF-α in SAMP6 mice compared to SAMR1 mice ($p < 0.05$, Fig. 2A). Additionally, the expression levels of the Mg^{2+} transporter mitochondrial RNA splicing 2 protein (MRS2) and transient receptor potential cation channel subfamily M member 6 (TRPM6) ($p < 0.05$) were markedly decreased in the olfactory epithelium of SAMP6 mice (Fig. 2B). The expression of angiotensin-related factors, AGT, Ang II, and angiotensin II type 1 receptor (AT1R) was significantly downregulated in aged SAMP6 mice ($p < 0.05$, Fig. 2C). Finally, we assessed the expression of mitochondrial apoptosis-related proteins. In the olfactory epithelium of SAMP6 mice, B-cell leukemia/lymphoma 2 (Bcl-2) expression was reduced, while the expression of Bcl-2-associated X protein (Bax), caspase-3, and caspase-9 was significantly elevated ($p < 0.05$, Fig. 2D), suggesting enhanced apoptotic activity in the olfactory epithelium of aged SAMP6 mice.

$MgSO_4$ Reduced the Damage to MOE Cells Caused by AGT Knockdown

To further elucidate the role of AGT in olfactory epithelial cells, we constructed three AGT-targeting shRNAs and transfected them into MOE cells. The results exhibited that all three shRNAs significantly downregulated the expression of *Agt* in MOE cells, with shRNA-2 demonstrating the most effective knockdown and thus was selected for subsequent experiments ($p < 0.05$, Fig. 3A). The optimal dose of $MgSO_4$ was determined using a CCK-8 assay. The findings revealed that lower doses of $MgSO_4$ enhanced MOE cell viability, while higher doses led to reduced viability. Therefore, a concentration of 1.25 µg/mL of $MgSO_4$ was used for MOE cell treatment in the following experiments ($p < 0.05$, Fig. 3B).

Knockdown of AGT significantly decreased MOE cell viability, which was subsequently restored following $MgSO_4$ treatment ($p < 0.05$, Fig. 3C). Additionally, the SOD level in the culture supernatant of the sh-AGT group was significantly reduced, while the levels of ROS, MDA, IL-1β, and TNF-α were significantly increased ($p < 0.05$, Fig. 3D,E). In the sh-AGT group, JC-1 monomer fluorescence intensity was increased, and JC-1 aggregate fluorescence was decreased ($p < 0.05$, Fig. 3F), suggesting a reduction in MMP and impaired mitochondrial function. Notably, $MgSO_4$ intervention alleviated the inflammation, oxidative stress, and mitochondrial dysfunction induced by AGT knockdown in MOE cells.

$MgSO_4$ Alleviated Alterations in Protein Expression Related to AGT, Mg^{2+} Transport, Inflammation, and Mitochondrial Apoptosis in MOE Cells Following AGT Knockdown

Next, we assessed the expression of markers associated with inflammation, AGT, Mg^{2+} transport, and mitochondrial apoptosis in the MOE cell groups that were treated differently. Consistent with the *in vivo* and ELISA results, AGT knockdown significantly increased IL-1β and TNF-α expression in MOE cells ($p < 0.05$, Fig. 4A) while decreasing the expression of Mg^{2+} transporter proteins MRS2 and TRPM6 ($p < 0.05$, Fig. 4B), as well as AGT, Ang II, AT1R ($p < 0.05$, Fig. 4C). These effects of AGT silencing were markedly inhibited by $MgSO_4$ treatment, as evidenced by the suppression of inflammatory cytokine expression and partial restoration of AGT and Mg^{2+}

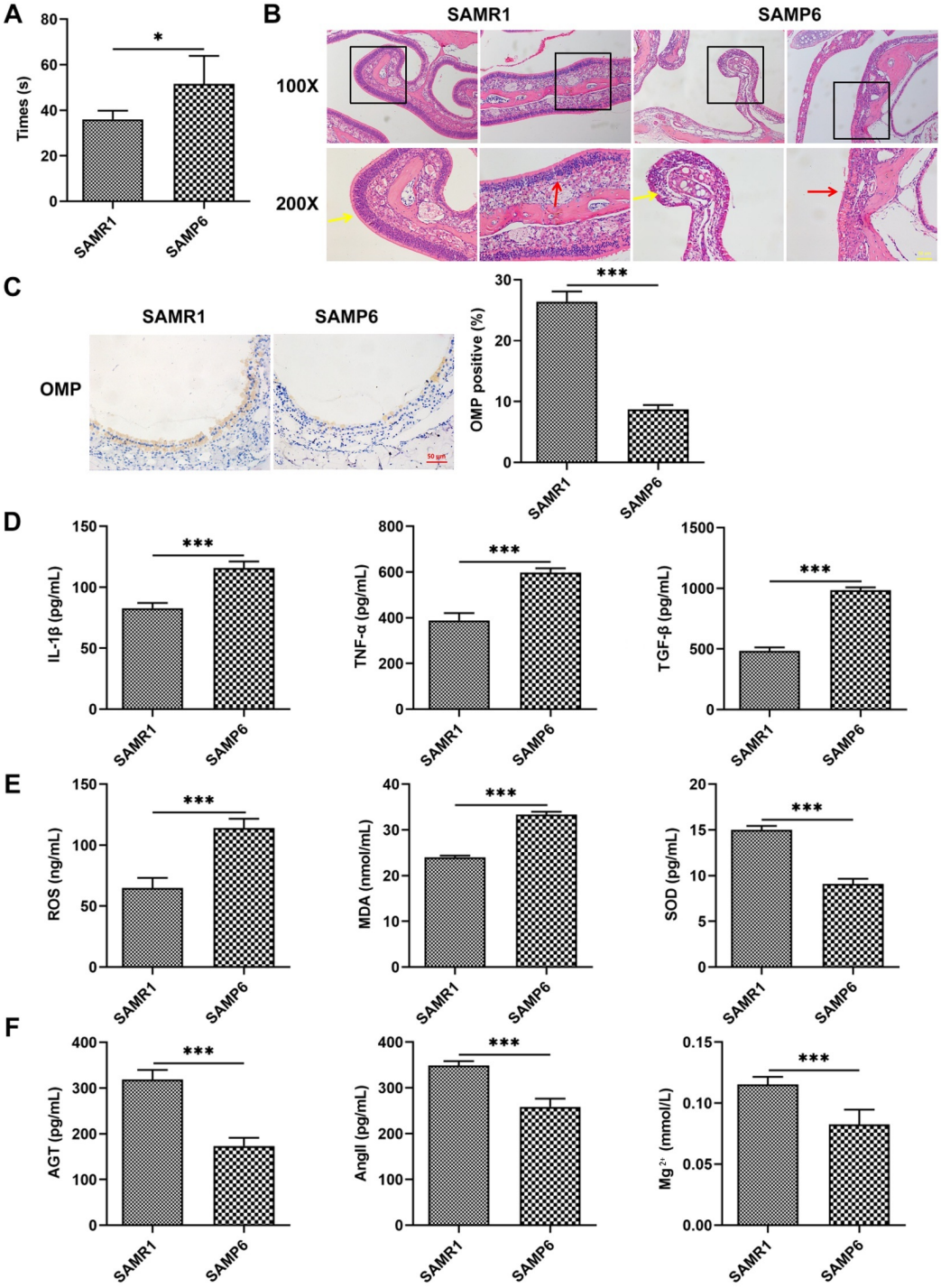

Fig. 1. SAMP6 mice showed impaired olfactory function associated with altered serum AGT, Mg^{2+}, and markers of inflammation and oxidative stress. (A) SAMP6 mice required significantly more time to locate buried food in the olfactory foraging test. (B) H&E staining revealed atrophy of the olfactory mucosal epithelium in SAMP6 mice compared to SAMR1 controls (scale bar = 50 µm). (C) IHC showed markedly reduced expression of the olfactory marker protein (OMP) in SAMP6 mice (scale bar = 50 µm). (D–F) Serum analysis revealed increased levels of IL-1β, TNF-α, TGF-β, ROS, and MDA, and decreased SOD in SAMP6 mice compared to SAMR1 mice, suggesting enhanced inflammation and oxidative stress. Serum AGT, Ang II, and Mg^{2+} levels were also reduced, suggesting compromised magnesium homeostasis (n = 6, SAMP6 and age-matched SAMR1 mice). *$p < 0.05$, ***$p < 0.001$. SAMP6, senescence-accelerated mouse prone 6; SAMR1, senescence accelerated mouse resistant 1; AGT, angiotensinogen; IHC, immunohistochemistry; IL-1β, interleukin-1 beta; TNF-α, tumor necrosis factor alpha; TGF-β, transforming growth factor beta; ROS, reactive oxygen species; MDA, malondialdehyde; SOD, superoxide dismutase; Ang II, angiotensin II.

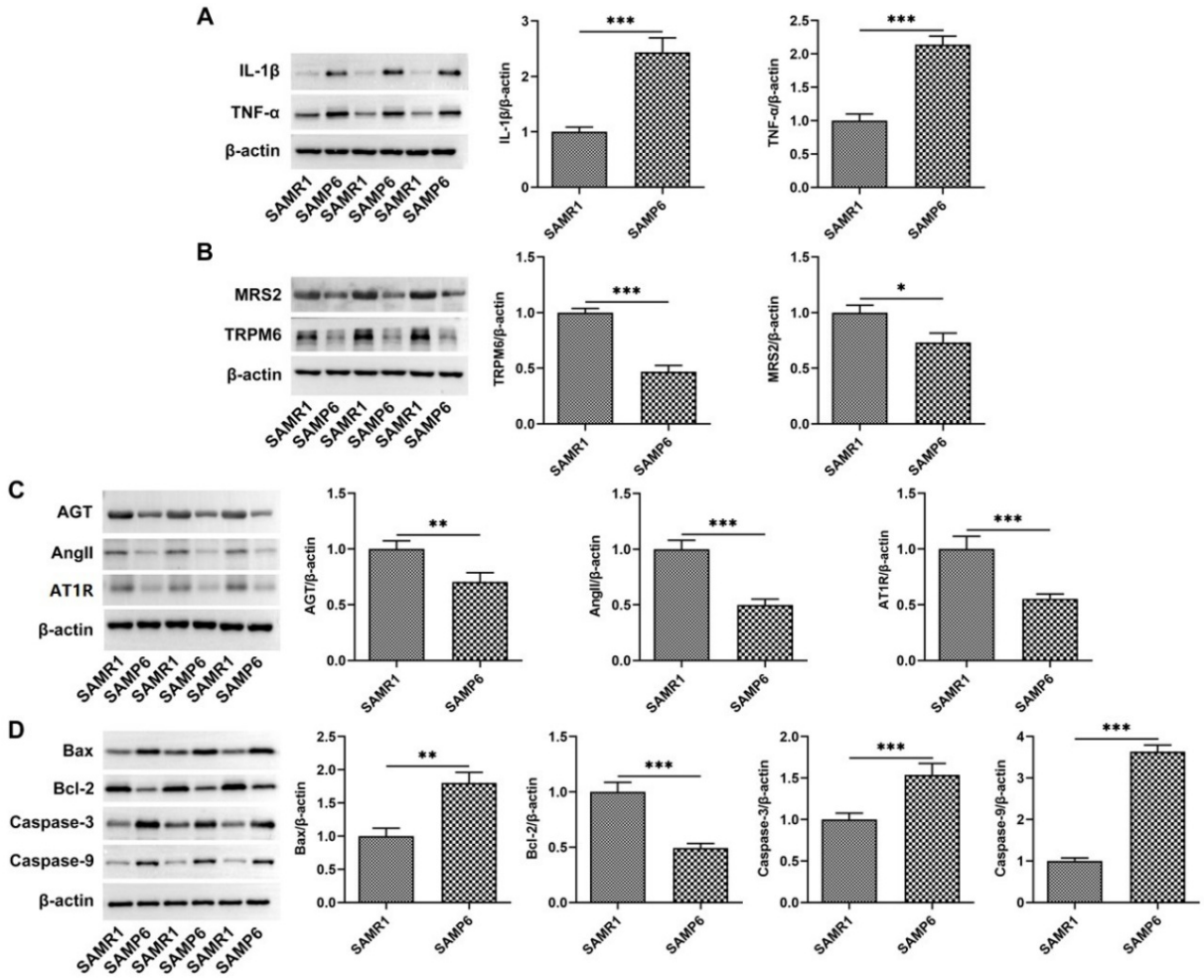

Fig. 2. SAMP6 mice showed altered expression of proteins associated with AGT signaling, Mg^{2+} transport, inflammation, and mitochondrial apoptosis in the olfactory epithelium. (A–D) Western blotting of olfactory epithelium tissue revealed significantly elevated expression of IL-1β and TNF-α in SAMP6 compared to SAMR1. Expression magnesium transporters MRS2 and transient receptor potential cation channel subfamily M member 6 (TRPM6), as well as AGT, Ang II, and AT1R, were significantly reduced in SAMP6. Markers of mitochondrial apoptosis were also decreased, whereas Bax, caspase-3, and caspase-9 levels were increased in SAMP6 mice (n = 3). *$p < 0.05$, **$p < 0.01$, ***$p < 0.001$. AT1R, angiotensin II type 1 receptor; MRS2, mitochondrial RNA splicing 2 protein.

transporter proteins in the sh-AGT+$MgSO_4$ group of MOE cells. Additionally, AGT knockdown significantly upregulated the expression of Bax, caspase-3, and caspase-9, while downregulating Bcl-2 expression in MOE cells ($p < 0.05$, Fig. 4D). Notably, $MgSO_4$ treatment reversed these changes in apoptosis-related proteins, suggesting that AGT knockdown-induced mitochondrial apoptosis in MOE cells.

Discussion

Smell is one of the five primary sensory functions of the human body, and odor recognition influences emotions, appetite, and even the ability to detect danger in certain situations [4]. Olfactory dysfunction poses a challenge to human health and overall quality of life. Its occurrence is usually the result of multiple pathophysiological processes, and the limited understanding of its mechanisms has hindered the development of standardized treatment strategies [17]. In this study, we investigated the potential role and mechanism of the *Agt* gene in olfactory dysfunction through *in vivo* and *in vitro* experiments. Preliminary findings suggest that reduced AGT expression in olfactory epithelial cells leads to cell inflammation, oxidative stress, and mitochondrial apoptosis by inhibiting Mg^{2+} uptake, thereby potentially contributing to olfactory dysfunction.

Ageing is a major contributor to the decline in olfactory function. The SAMP6 mouse model, characterized by accelerated ageing, was used in this study. We observed that SAMP6 mice required more time to locate food during the olfactory foraging test compared to SAMR1 mice. Olfactory marker protein (OMP), expressed in mature olfac-

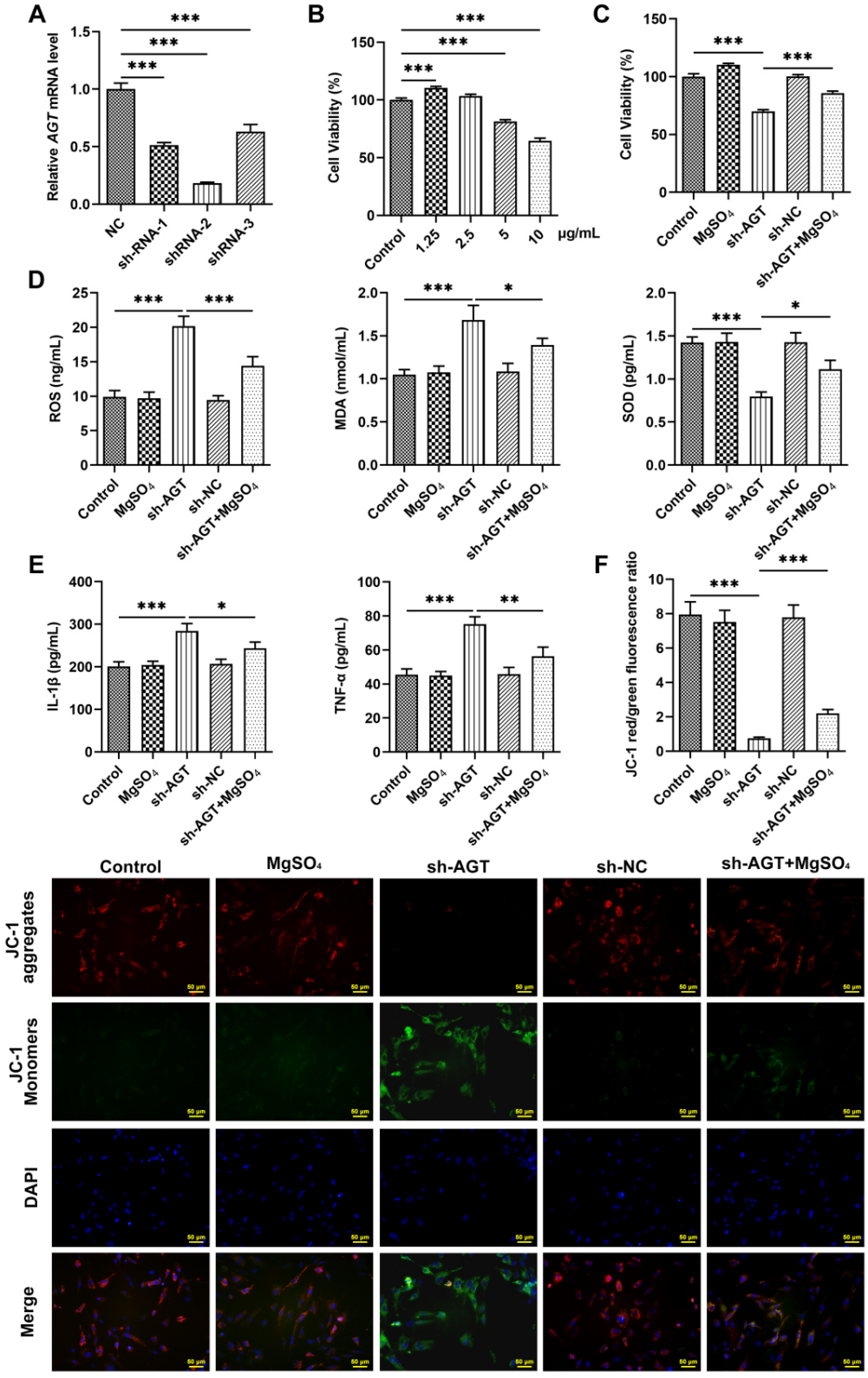

Fig. 3. $MgSO_4$ reduced AGT knockdown-induced damage in MOE cells. (A) RT-PCR analysis of *Agt* mRNA expression following transfection with three sh-RNAs compared to sh-NC in MOE cells (n = 3). (B) Dose-response screening for $MgSO_4$ using the Cell Counting Kit-8 (CCK-8) assay (n = 3). (C) Cell viability under *Agt* knockdown with or without 1.25 mg/mL $MgSO_4$ treatment (n = 3). (D,E) Levels of ROS, MDA, SOD, IL-1β, and TNF-α in culture supernatants (n = 3). (F) JC-1 staining to assess mitochondrial membrane potential. *$p < 0.05$, **$p < 0.01$, ***$p < 0.001$. MOE, mouse olfactory epithelial.

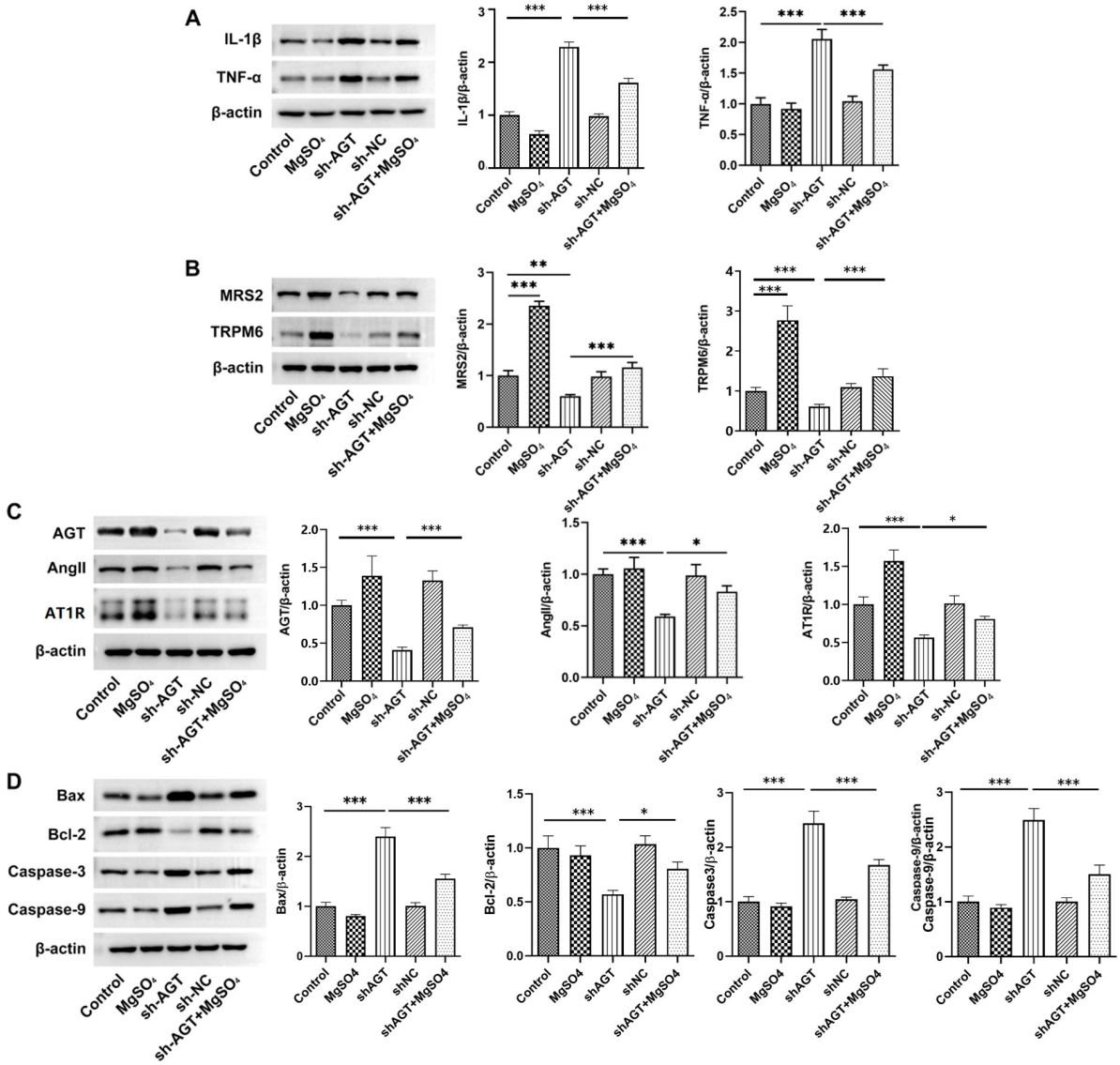

Fig. 4. $MgSO_4$ alleviated AGT knockdown-induced alterations in functional protein expression in MOE cells. Western blot of MOE cells for (A) IL-1β and TNF-α, (B) MRS2 and TRPM6, (C) AGT, Ang II, and AT1R, and (D) Bax, Bcl-2, caspase-3, and caspase-9. β-actin served as the loading control (n = 3). *$p < 0.05$, **$p < 0.01$, ***$p < 0.001$.

tory receptor neurons, plays a key role in regulating olfactory sensitivity and axon targeting [18]. IHC results showed significantly reduced OMP expression in the olfactory epithelium of SAMP6 mice. In addition, levels of inflammation, oxidative stress, and mitochondrial apoptosis-related markers were significantly upregulated in both the olfactory epithelium and serum of SAMP6 mice compared with SAMR1 mice. These findings suggest that age-associated olfactory dysfunction may be closely related to systemic and local inflammatory responses, oxidative stress, and mitochondrial apoptosis in the body.

Agt encodes angiotensinogen, a key component of the RAS. Hyposmia is a characteristic symptom observed in COVID-19. Previous studies have shown that the SARS-CoV-2 virus utilizes ACE2 receptors to gain entry into human cells. Notably, ACE2 is highly expressed in olfactory epithelial cells, which may partly explain the olfactory dysfunction observed in COVID-19 patients [19,20]. In addition, ACE2 knockout in mice results in morphological abnormalities in the olfactory center and olfactory dysfunction [21]. These observations suggest a potential association between RAS activity and olfactory function, especially under pathological conditions such as viral infection. However, further investigation is needed to clarify the role of the RAS system in age-related or infection-induced hyposmia. In the present study, we observed that levels of AGT, Ang II, and AT1R were reduced in serum and olfactory epithelial tissues of ageing mice, suggesting that the RAS system mediates age-related hyposmia.

Magnesium is one of the most essential micronutrients for life and is involved in the regulation of human immunity, bone growth, neuromuscular excitability, gastrointestinal function, and hormonal balance [22]. Similarly, recent study has demonstrated that low magnesium status is associated with increased severity of COVID-19 outcomes and with disease-related loss of smell and taste [23]. In the present study, we observed reduced serum magnesium levels in ageing mice, accompanied by decreased expression of Mg^{2+} transporters MRS2 and TRPM6 in the olfactory epithelium. These findings suggest that the age-related decline in olfactory function may be related to magnesium deficiency within the olfactory epithelium. Downregulation of AGT, MRS2, and TRPM6, along with reduced magnesium levels in ageing mice, raises the question of whether a correlation exists between *Agt* expression and magnesium homeostasis. This potential association warrants further investigation. Through *in vitro* experiments, we further observed that the expression of MRS2 and TRPM6 was reduced in olfactory epithelial cells following *Agt* knockdown, suggesting that AGT deficiency impairs Mg^{2+} uptake. In addition, supplementation with magnesium sulfate attenuated the inflammatory response, oxidative stress, and mitochondrial apoptosis induced by *Agt* knockdown in olfactory epithelial cells.

Mechanistically, diminished *Agt* expression may decrease Ang II levels, thereby weakening the RAS–mediated regulation of Mg^{2+} homeostasis. Notably, Herencia *et al.* [13] reported that Ang II modulates magnesium influx in vascular smooth muscle cells, indicating a broader regulatory role of RAS in Mg^{2+} transport. In the context of the olfactory epithelium, low *Agt* expression may compromise the expression or activity of Mg^{2+} transporters such as TRPM6 and MRS2, leading to intracellular Mg^{2+} deficiency. This deficiency, in turn, may heighten inflammation and oxidative stress, both of which are harmful to sensory receptor cells. Magnesium is increasingly recognized as a critical micronutrient for multiple sensory processes, including olfaction [24]. Collectively, these findings support the hypothesis that robust *Agt* signaling and adequate Mg^{2+} uptake are essential for maintaining olfactory epithelial integrity and that disruption of either pathway may contribute to the pathophysiology of olfactory dysfunction.

Despite the promising findings, several considerations warrant attention. First, we did not include additional behavioral assays (e.g., olfactory discrimination tests) that could better distinguish between pure olfactory deficits and potential motor or cognitive influences. Incorporating such tests in future studies could enhance the specificity of our findings. Second, although our knockdown strategy provides strong evidence of AGT's role, complementary overexpression experiments are needed to determine whether restoring AGT levels can reverse the observed phenotypes. Finally, while our sample sizes were sufficient to detect significant effects, larger cohorts would improve statistical power and enhance the generalizability of our conclusions. These considerations highlight important directions for future research aimed at translating our observations into broader biological insights and potential therapeutic strategies.

In conclusion, the present study demonstrates that reduced expression of AGT in olfactory epithelial cells is associated with low intracellular magnesium levels and cellular damage. AGT may influence inflammation, oxidative stress, and mitochondrial apoptosis by regulating magnesium ion uptake in these cells. These findings may provide a basis and guidance for developing diagnostic and therapeutic approaches for sinonasal olfactory dysfunction, especially among middle-aged and elderly patients.

Conclusion

Our study reveals that reduced AGT expression impairs Mg^{2+} uptake in olfactory epithelial cells, leading to inflammation, oxidative stress, and mitochondrial apoptosis, factors that contribute to age-related olfactory dysfunction. Restoration of Mg^{2+} levels through $MgSO_4$ supplementation partially rescues these phenotypes, highlighting AGT and Mg^{2+} homeostasis as potential therapeutic targets for preventing or treating olfactory disorders in the ageing population.

Availability of Data and Materials

The datasets used and/or analyzed in the current study are available from the corresponding author upon reasonable request.

Author Contributions

DW and WL conceived and designed the experiments. DW and JY performed the experimental operation, data preservation, and literature search. BL performed the data analysis and visualization. WL provided technical support and supervision. DW wrote the first draft of the manuscript, and WL revised it. All authors have been involved in revising it critically for important intellectual content. All authors read and approved the final manuscript. All authors have participated sufficiently in the work and agreed to be accountable for all aspects of the work.

Ethics Approval and Consent to Participate

All animal experiments were complied with the ARRIVE guidelines and carried out in accordance with the National Institutes of Health guide for the care and use of Laboratory animals (NIH Publications No. 8023, revised 1978). All animal experiments were approved by the Institutional Animal Care and Use Committee of the Second Affiliated Hospital of Chongqing Medical University (approval number: IACUC-SAHCQMU-2023-0070).

Acknowledgment

The authors would like to thank all staff who contributed to this study.

Funding

This research received no external funding.

Conflict of Interest

The authors declare no conflict of interest.

References

[1] Scangas GA, Bleier BS. Anosmia: Differential diagnosis, evaluation, and management. American Journal of Rhinology & Allergy. 2017; 31: 3–7. https://doi.org/10.2500/ajra.2017.31.4403.

[2] Ubeda-Bañon I, Saiz-Sanchez D, Flores-Cuadrado A, Rioja-Corroto E, Gonzalez-Rodriguez M, Villar-Conde S, *et al*. The human olfactory system in two proteinopathies: Alzheimer's and Parkinson's diseases. Translational Neurodegeneration. 2020; 9: 22. https://doi.org/10.1186/s40035-020-00200-7.

[3] Mignot C, Nahrath P, Sinding C, Hummel T. Older and Young Adults Experience Similar Long-Term Olfactory Habituation. Chemical Senses. 2021; 46: bjaa080. https://doi.org/10.1093/chemse/bjaa080.

[4] Boesveldt S, Postma EM, Boak D, Welge-Luessen A, Schöpf V, Mainland JD, *et al*. Anosmia-A Clinical Review. Chemical Senses. 2017; 42: 513–523. https://doi.org/10.1093/chemse/bjx025.

[5] Jankowski R, Nguyen DT, Russel A, Toussaint B, Gallet P, Rumeau C. Chronic nasal dysfunction. European Annals of Otorhinolaryngology, Head and Neck Diseases. 2018; 135: 41–49. https://doi.org/10.1016/j.anorl.2017.11.006.

[6] Aragona M, Porcino C, Guerrera MC, Montalbano G, Laurà R, Levanti M, *et al*. Localization of BDNF and Calretinin in Olfactory Epithelium and Taste Buds of Zebrafish (*Danio rerio*). International Journal of Molecular Sciences. 2022; 23: 4696. https://doi.org/10.3390/ijms23094696.

[7] Kandemirli SG, Altundag A, Yildirim D, Tekcan Sanli DE, Saatci O. Olfactory Bulb MRI and Paranasal Sinus CT Findings in Persistent COVID-19 Anosmia. Academic Radiology. 2021; 28: 28–35. https://doi.org/10.1016/j.acra.2020.10.006.

[8] Yan CH, Faraji F, Prajapati DP, Ostrander BT, DeConde AS. Self-reported olfactory loss associates with outpatient clinical course in COVID-19. International Forum of Allergy & Rhinology. 2020; 10: 821–831. https://doi.org/10.1002/alr.22592.

[9] Al-Saigh NN, Harb AA, Abdalla S. Receptors Involved in COVID-19-Related Anosmia: An Update on the Pathophysiology and the Mechanistic Aspects. International Journal of Molecular Sciences. 2024; 25: 8527. https://doi.org/10.3390/ijms25158527.

[10] Kerns SL, Fachal L, Dorling L, Barnett GC, Baran A, Peterson DR, *et al*. Radiogenomics Consortium Genome-Wide Association Study Meta-Analysis of Late Toxicity After Prostate Cancer Radiotherapy. Journal of the National Cancer Institute. 2020; 112: 179–190. https://doi.org/10.1093/jnci/djz075.

[11] Chrysanthopoulou A, Gkaliagkousi E, Lazaridis A, Arelaki S, Pateinakis P, Ntinopoulou M, *et al*. Angiotensin II triggers release of neutrophil extracellular traps, linking thromboinflammation with essential hypertension. JCI Insight. 2021; 6: e148668. https://doi.org/10.1172/jci.insight.148668.

[12] González-Amor M, García-Redondo AB, Jorge I, Zalba G, Becares M, Ruiz-Rodríguez MJ, *et al*. Interferon-stimulated gene 15 pathway is a novel mediator of endothelial dysfunction and aneurysms development in angiotensin II infused mice through increased oxidative stress. Cardiovascular Research. 2022; 118: 3250–3268. https://doi.org/10.1093/cvr/cvab321.

[13] Herencia C, Rodríguez-Ortiz ME, Muñoz-Castañeda JR, Martinez-Moreno JM, Canalejo R, Montes de Oca A, *et al*. Angiotensin II prevents calcification in vascular smooth muscle cells by enhancing magnesium influx. European Journal of Clinical Investigation. 2015; 45: 1129–1144. https://doi.org/10.1111/eci.12517.

[14] Nicolau LAD, Magalhães PJC, Vale ML. What would Sérgio Ferreira say to your physician in this war against COVID-19: How about kallikrein/kinin system? Medical Hypotheses. 2020; 143: 109886. https://doi.org/10.1016/j.mehy.2020.109886.

[15] Méndez-García LA, Escobedo G, Minguer-Uribe AG, Viurcos-Sanabria R, Aguayo-Guerrero JA, Carrillo-Ruiz JD, *et al*. Role of the renin-angiotensin system in the development of COVID-19-associated neurological manifestations. Frontiers in Cellular Neuroscience. 2022; 16: 977039. https://doi.org/10.3389/fncel.2022.977039.

[16] Henkin RI. Drug-induced taste and smell disorders. Incidence, mechanisms and management related primarily to treatment of sensory receptor dysfunction. Drug Safety. 1994; 11: 318–377. https://doi.org/10.2165/00002018-199411050-00004.

[17] Nota J, Takahashi H, Hakuba N, Hato N, Gyo K. Treatment of neural anosmia by topical application of basic fibroblast growth factor-gelatin hydrogel in the nasal cavity: an experimental study in mice. JAMA Otolaryngology– Head & Neck Surgery. 2013; 139: 396–400. https://doi.org/10.1001/jamaoto.2013.92.

[18] Nakashima N, Nakashima A, Nakashima K, Takano M. Olfactory marker protein contains a leucine-rich domain in the Ω-loop important for nuclear export. Molecular Brain. 2022; 15: 89. https://doi.org/10.1186/s13041-022-00973-0.

[19] Chen M, Shen W, Rowan NR, Kulaga H, Hillel A, Ramanathan M, Jr, *et al*. Elevated ACE-2 expression in the olfactory neuroepithelium: implications for anosmia and upper respiratory SARS-CoV-2 entry and replication. The European Respiratory Journal. 2020; 56: 2001948. https://doi.org/10.1183/13993003.01948-2020.

[20] Brann DH, Tsukahara T, Weinreb C, Lipovsek M, Van den Berge K, Gong B, *et al*. Non-neuronal expression of SARS-CoV-2 entry genes in the olfactory system suggests mechanisms underlying COVID-19-associated anosmia. Science Advances. 2020; 6: eabc5801. https://doi.org/10.1126/sciadv.abc5801.

[21] Mahajan S, Sen D, Sunil A, Srikanth P, Marathe SD, Shaw K, *et al*. Knockout of angiotensin converting enzyme-2 receptor leads to morphological aberrations in rodent olfactory centers and dysfunctions associated with sense of smell. Frontiers in Neuroscience. 2023; 17: 1180868. https://doi.org/10.3389/fnins.2023.1180868.

[22] Fanni D, Gerosa C, Nurchi VM, Manchia M, Saba L, Coghe F, *et al*. The Role of Magnesium in Pregnancy and in Fetal Programming of Adult Diseases. Biological Trace Element Research. 2021; 199: 3647–3657. https://doi.org/10.1007/s12011-020-02513-0.

[23] Guerrero-Romero F, Micke O, Simental-Mendía LE, Rodríguez-Morán M, Vormann J, Iotti S, *et al*. Importance of Magnesium Status in COVID-19. Biology. 2023; 12: 735. https://doi.org/10.3390/biology12050735.

[24] Fiorentini D, Cappadone C, Farruggia G, Prata C. Magnesium: Biochemistry, Nutrition, Detection, and Social Impact of Diseases Linked to Its Deficiency. Nutrients. 2021; 13: 1136. https://doi.org/10.3390/nu13041136.